Biochimica et Biophysica Acta 1859 (2017) 1796–1804

Contents lists available at ScienceDirect

Biochimica et Biophysica Acta

journal homepage: www.elsevier.com/locate/bbamem

Investigations into the killing activity of an antimicrobial peptide active against extensively antibiotic-resistant *K. pneumon iae* and *P. aeruginosa*

Hessel van der Weide [a,1], Jlenia Brunetti [b,1], Alessandro Pini [b], Luisa Bracci [b], Chiara Ambrosini [b], Pietro Lupetti [c], Eugenio Paccagnini [c], Mariangela Gentile [c], Andrea Bernini [d], Neri Niccolai [d], Denise Vermeulen-de Jongh [a], Irma A.J.M. Bakker-Woudenberg [a], Wil H.F. Goessens [a], John P. Hays [a], Chiara Falciani [b,e,*]

[a] Department of Medical Microbiology & Infectious Diseases, Erasmus University Medical Center, Rotterdam, The Netherlands
[b] Department of Medical Biotechnology, University of Siena, Italy
[c] Department of Life Sciences, University of Siena, Italy
[d] Department of Biotechnology, Chemistry and Pharmacy, University of Siena, Italy
[e] Setlance srl, Research and Development Department, Siena, Italy

ARTICLE INFO

Article history:
Received 1 March 2017
Received in revised form 10 May 2017
Accepted 1 June 2017
Available online 3 June 2017

Keywords:
Antimicrobial peptide
Membrane interactions
Resistance to antimicrobials
NMR
Electron microscopy
Circular dichroism

ABSTRACT

SET-M33 is a multimeric antimicrobial peptide active against Gram-negative bacteria *in vitro* and *in vivo*. Insights into its killing mechanism could elucidate correlations with selectivity.
SET-M33 showed concentration-dependent bactericidal activity against colistin-susceptible and resistant isolates of *P. aeruginosa* and *K. pneumoniae*. Scanning and transmission microscopy studies showed that SET-M33 generated cell blisters, blebs, membrane stacks and deep craters in *K. pneumoniae* and *P. aeruginosa* cells. NMR analysis and CD spectra in the presence of sodium dodecyl sulfate micelles showed a transition from an unstructured state to a stable α-helix, driving the peptide to arrange itself on the surface of micelles.
SET-M33 kills Gram-negative bacteria after an initial interaction with bacterial LPS. The molecule becomes then embedded in the outer membrane surface, thereby impairing cell function. This activity of SET-M33, in contrast to other similar antimicrobial peptides such as colistin, does not generate resistant mutants after 24 h of exposure, non-specific interactions or toxicity against eukaryotic cell membranes, suggesting that SET-M33 is a promising new option for the treatment of Gram-negative antibiotic-resistant infections.

1. Introduction

Extensive use of broad-spectrum antibiotics has led to the development and spread of extensively antibiotic-resistant strains of bacteria, making antimicrobial resistance a global problem. Antibiotic-resistant bacteria kill 25,000 people in the EU every year. Infections such as urinary tract infections [1], pneumonia [2] and septicemia [3] are increasingly associated with multi-drug resistant Gram-negative bacteria in all regions of the world [4]. These antibiotic-resistant bacteria generally cause infections associated with increased risk of poor clinical outcome and mortality compared to non-resistant strains of the same bacteria [5]. The World Health Organization warns that antimicrobial resistance is an increasingly serious threat to global public health and calls for action across all government sectors and society [6] to avoid a dreaded "post-antibiotic" era.

A recent rekindling of antibiotic research has shown that the antimicrobial peptide class of antibiotics is particularly promising for use against infections caused by multidrug-resistant microorganisms [7–9]. Antimicrobial peptides (AMPs) are an important component of the natural defenses of most living organisms, and >2500 AMPs have been registered in the Antimicrobial Peptide Database (http://aps.unmc.edu/AP/main.php) [10]. However, despite their desirable characteristics, antimicrobial peptides have had limited pharmaceutical development due to their toxicity, instability and manufacturing costs, and therefore only a few AMPs have actually been approved for clinical use [11–12].

The most common mechanism of antimicrobial killing by antimicrobial peptides is disruption of the cytoplasmic membrane, for example by pore formation, which is rather non-specific but highly efficient [13–15]. Alternative mechanisms of action include peptide translocation into the cytoplasm where the antibiotic interferes with bacterial metabolic processes, such as protein synthesis or DNA replication, while

* Corresponding author at: Department of Medical Microbiology & Infectious Diseases, Erasmus University Medical Center, Rotterdam, The Netherlands.
E-mail address: chiara.falciani@unisi.it (C. Falciani).
[1] The two authors contributed equally.

http://dx.doi.org/10.1016/j.bbamem.2017.06.001

other peptides are known to interact directly with specific membrane components [16–18]. In particular, cationic AMPs have been demonstrated to induce anionic lipid clustering which appears to arrest bacterial growth or trigger cell death [19–20].

SET-M33 is an antimicrobial peptide that has been extensively studied in recent years [21–25]. It is a cationic non-natural peptide built in a branched form (Fig. 1) that makes it more resistant to degradation in biological fluids [26]. SET-M33 has shown efficacy against a number of Gram-negative multi-drug and extensively drug-resistant clinical isolates [21,24]. It has also shown acceptable toxicity in human cells and in mice [22], as well as anti-inflammatory activity [23]. Nevertheless, its mechanism of action has not yet been researched in depth. In this study we used different techniques to study the mechanism of action of SET-M33 against two Gram-negative bacterial species, *K. pneumoniae* and *P. aeruginosa*: 1) bacterial killing kinetics over time to see concentration-dependency and onset of resistance; 2) electron microscopy imaging of treated bacteria to visualize membrane disturbance; 3) hemolytic activity to assess eukaryotic cell toxicity and 4) NMR and circular dichroism to study the structure of the peptides in the presence of micelles and their ability to stabilize in a facial amphiphilic helix.

2. Materials and methods

2.1. Peptide synthesis

All peptides were prepared by solid-phase synthesis through standard Fmoc chemistry using a Syro multiple peptide synthesizer (MultiSynTech, Witten, Germany). Side chain protecting groups were 2,2,4,6,7-pentamethyldihydrobenzofuran-5-sulfonyl for R, t-butoxycarbonyl for K and t-butyl for S (Iris Biotech GmbH, Marktredwitz, Germany). The final products were cleaved from the solid support, de-protected by treatment with TFA containing triisopropylsilane and water (95/2.5/2.5), and precipitated with diethyl ether. Final peptide purity and identity was confirmed by reverse-phase chromatography on a Phenomenex Jupiter C18 analytical column (300 Å, 250 × 4.6 mm) and by mass spectrometry.

Q-33 (linear peptide, QKKIRVRLSA) was produced on TentaGel S RAM resin (Iris Biotech GmbH, Marktredwitz, Germany). The crude peptide, released as amide, was purified by reverse-phase chromatography on a Phenomenex Jupiter C18 column (300 Å, 250 × 10 mm), in a linear gradient, using 0.1% TFA/water as eluent A and acetonitrile as eluent B (from 99% to 50% of A in 30 min). The compound was characterized on a MALDI-TOF mass spectrometer (Ultraflex III Bruker Daltonics): QKKIRVRLSA-NH_2, MALDI-MS: 1198.97 [M + H]+; RP-HPLC: t_R = 19.62 min, purity > 99%.

SET-M33 (tetrabranched peptide, $(KKIRVRLSA)_4K_2K\beta A$-OH) was synthesized on a Fmoc4-Lys2-Lys-β-Ala Wang resin (Iris Biotech GmbH, Marktredwitz, Germany). The crude peptide, released as carboxylic acid, was purified by reverse-phase chromatography on a Phenomenex Jupiter C18 analytical column (300 Å, 250 × 10 mm) in a linear gradient, using water with 0.1% TFA as eluent A and acetonitrile as eluent B (from 82% to 75% of A in 60 min). The purified peptide was obtained as a trifluoroacetate salt and exchanged to acetate using a quaternary ammonium resin (AG1-X8, 100–200 mesh, 1.2 meq/mL capacity). The resin-to-peptide ratio was 2000:1, resin and peptide were stirred for 1 h, the resin filtered off, washed extensively and the peptide recovered and freeze-dried. The compound was characterized on a MALDI-TOF mass spectrometer (Ultraflex III Bruker Daltonics): $(KKIRVRLSA)_4K_2K\beta A$-OH MALDI-MS: 4682.48 [M + H]+; RP-HPLC: t_R = 21.10 min, purity > 99%. SET-M33 solubility, water ≥ 20 mg/mL, saline ≥ 20 mg/mL, PBS ≥ 15 mg/mL.

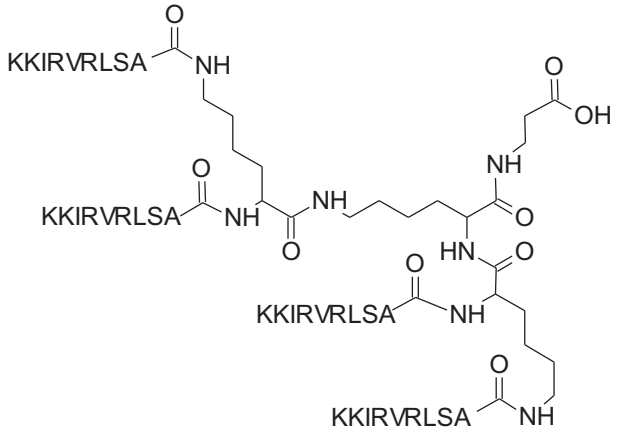

Fig. 1. Structure of SET-M33.

2.2. Selection of colistin-resistant mutants of K. pneumoniae R-DYK 4861 and P. aeruginosa B-162

K. pneumoniae R-DYK 4861 and *P. aeruginosa* B-162 were both extensively antibiotic-resistant clinical isolates and colistin-susceptible. Colistin-resistant mutants of both strains were obtained by step-wise serial passages of bacterial strains [27] in BBL™ Mueller Hinton II (MH-II) broth (Becton, Dickinson Benelux N.V., Erembodegem, Belgium) containing colistin concentrations in the range 2–64 mg/L (colistin sulfate, Sigma-Aldrich Chemie BV, Zwijndrecht, the Netherlands). This involved sub-culturing 100 μL of overnight culture of the bacteria (grown in MH-II broth) into MH-II broth containing 2 mg/L colistin and incubating overnight at 35 °C. In subsequent steps 100 μL of overnight culture was sub-cultured into MH-II broth containing two-fold increases in the concentration of colistin until the highest colistin concentration of 64 mg/L was achieved. Finally, 100 μL volumes were sub-cultured onto solid MH-II medium (Becton, Dickinson Benelux N.V., Erembodegem, Belgium). Colistin-resistant colonies were then characterized phenotypically using VITEK® 2.

2.3. Phenotypic characterization of bacterial isolates

Phenotypic characterization of *K. pneumoniae* B-DYK 4861 and *P. aeruginosa* B-162 isolates and their colistin-resistant mutants was performed by determining their susceptibility for a panel of 18 different antibiotics from the main classes of antibiotics using the VITEK® 2 antimicrobial identification system (BioMérieux Benelux BV, Zaltbommel, The Netherlands) and AST-N140 cards (Vitek AMS). Interpretation of antimicrobial susceptibility was based on EUCAST 2017 guidelines [28] (Table 1S Supplementary data).

2.4. Antimicrobial susceptibility of bacterial isolates – MIC assay

Antimicrobial susceptibility was assessed by determining the Minimum Inhibitory Concentration (MIC) of SET-M33 and colistin using the broth microdilution technique according to 2017 EUCAST guidelines. The MIC assay measures visible inhibition of bacterial growth after 24 h exposure of bacteria to antibiotic in MH-II broth. The two-fold antibiotic concentration range used for SET-M33 and colistin was 0.063–64 mg/L.

2.5. Concentration- and time-dependent bactericidal activity of SET-M33 and colistin – TKK assay

The concentration- and time-dependent killing capacity of SET-M33 was determined using time-kill kinetic (TKK) assays, as previously described [29]. Briefly, stationary-phase MH-II broth cultures of *K. pneumoniae* R-DYK 4861 and *P. aeruginosa* B-162 were diluted in 25 mL MH-II broth until a density of approximately 7×10^5 colony forming units (CFU/mL) was achieved. Bacterial cultures were exposed to antimicrobial antibiotics at 2-fold increasing concentrations for 24 h

at 37 °C under shaking conditions at 96 rpm at 37 °C. Next, 1 mL samples were taken at 0, 1, 2, 4, 6 and 24 h of antibiotic exposure and centrifuged at 12500 ×*g* for 5 min to pellet the cells, which were then resuspended in sterile PBS. Agar plates were incubated for 24 h (*K. pneumoniae*) or 48 h (*P. aeruginosa*) at 37 °C in order to determine the number of CFU. The lower limit of quantification in this assay was 5 CFU/mL (log 0.7). For colistin-susceptible bacterial isolates, the two-fold antibiotic concentration range was 0.125–64 mg/L for SET-M33 and colistin alike. For colistin-resistant isolates, the two-fold antibiotic concentration range was 0.125–64 mg/L for SET-M33 and 1–512 mg/L for colistin. Flasks showing re-growth of bacteria after 24 h antibiotic exposure were examined for changes in antibiotic susceptibility using the antibiotic MIC assay described above, but with an antibiotic concentration range of 0.5–512 mg/L for the colistin-resistant isolates.

2.6. Sample preparation for electron microscopy

P. aeruginosa PAO1 and *K. pneumoniae* ATCC 13833 cells in logarithmic phase were resuspended at 2×10^8 CFU/mL in PBS and incubated with 1.5 μM SET-M33 at room temperature for 15, 30 and 60 min. The mixture was then centrifuged for 5 min at 10000 r.p.m.

2.7. Scanning electron microscopy

Centrifuged bacteria were resuspended in 500 μL PBS and a drop of liquid cell suspension was placed on untreated glass coverslip for five minutes. The coverslip was then fixed for immersion in 2.5% glutaraldehyde solution in phosphate buffer 0.1 M pH 7.2 (PB) for 2 h at 4 °C, washed in PB, postfixed in 1% OsO_4 in PB for 30 min at 4 °C, dehydrated in an ascending alcohol series, and dried in a Balzers CPD 030 CO_2 critical point dryer.

The coverslip was then mounted on an aluminum stub, coated with 20 nm gold in a Balzers MED010 sputtering device, and observed in a Philips XL20 scanning electron microscope with an electron accelerating voltage of 20 kV.

2.8. Transmission electron microscopy

Centrifuged bacteria were fixed in 2.5% glutaraldehyde solution in phosphate buffer 0.1 M pH 7.2 (PB) for 2 h at 4 °C, washed in PB, postfixed in 1% OsO_4 in PB for 30 min at 4 °C, dehydrated in an ascending alcohol series, incubated twice in propylene oxide and finally infiltrated and embedded in epon/araldite resin that was polymerized at 60 °C for 48 h.

Ultrathin sections (60 nm thick) were cut from samples on a Reichert-Jung Ultracut E ultramicrotome, mounted on 200-mesh copper grids, stained with uranyl acetate and lead citrate and observed in a FEI Technai G2 SPIRIT transmission electron microscope using an electron accelerating voltage of 100 kV under standard operating conditions.

2.9. Nuclear magnetic resonance

All NMR samples were prepared by dissolving lyophilized peptides in 500 μL H_2O/D_2O (95:5) to a final concentration of 1.0 mM, with the exception of SET-M33, which was dissolved to a final concentration of 0.25 mM. Since the resonance of N-terminus amide would be missed in aqueous media due to chemical exchange, the peptide sequence of the Q-33 peptide, bearing a leading glutamine [33–34], was used instead, allowing us to gain structural information on the Lys1 residue. Samples with micelles were prepared using 100 mM fully deuterated sodium dodecyl sulfate (SDS-d25, Cambridge Isotopes). Paramagnetic spectra were recorded with 2.5 mM Gd(III)(DTPA-BMA). All spectra were acquired on a Bruker DRX Avance spectrometer operating at 14.1 Tesla at a temperature of 298 K. Two-dimensional spectra were recorded by accumulating 32 FIDs for 512 experiments, digitalizing over 2048 points. Spectral width was set at 6000 Hz and repetition delay at 3 s. The mixing time for total correlation spectroscopy (TOCSY) and nuclear Overhauser spectroscopy (NOESY) spectra was set at 45/75 ms and 100/200/300 ms, respectively. All spectra were processed to a final size of 2048 by 1024 points. Peak assignment and integration were carried out with Sparky software (T. D. Goddard and D. G. Kneller, SPARKY 3, University of California, San Francisco) while calibration of NOE peak volumes, distance calculation and restrained torsion angle dynamics for structure calculation were performed using Dyana [30].

2.10. Circular dichroism

CD spectra were recorded at 25 °C with a Jasco 815 spectropolarimeter using quartz cells having a path length of 0.1-cm. SET-M33 (100 μM) or Q-33 (100 μM) were dissolved in pure water or 30 mM SDS. The results were processed with the application Spectra Manager II™ Suite.

2.11. Hemolytic activity

The ability of SET-M33 peptide to induce hemolysis of human red blood cells was assessed. Whole blood (EDTA) was centrifuged (1100 ×*g*) for 10 min. Red blood cells diluted 1:100 in PBS were incubated for 24 h at 37 °C in PBS with two-fold serial dilution of all peptides from 4 mg/L to 1.8 g/L. The absorbance of the supernatants was determined in a 96-well plate at 490 nm using a microplate reader. Date for 100% hemolysis was obtained by adding 0.1% Triton X-100 in water. The negative control was PBS. The hemolysis rate of each peptide was calculated with the following equation: Hemolysis (%) = $(A_{peptide} - A_{PBS}) / (A_{triton} - A_{PBS}) \times 100\%$; were A = absorbance.

2.12. FPLC-gel filtration

LPS from *P. aeruginosa* (ATCC 27316, Sigma Aldrich) and SET-M33 was gel-filtered on a Superdex 75 10/300 GL fast protein liquid chromatography column using an AKTA Purifier (GE Healthcare) in PBS pH 7.4. 100 μL of 2 g/L SET-M33 or 13 g/L LPS or 13 g/L LPS + 2 g/L SET-M33 was injected on a Superdex 75 10/300 GL column with a flow rate of 0.75 mL/min and absorbance was measured at 220 and 260 nm.

3. Results and discussion

The *K. pneumoniae* and *P. aeruginosa* isolates used in the following experiments were resistant to a wide range of beta-lactam antibiotics (penicillins, cephalosporins and carbapenems) including the 4th generation cephalosporin cefepime, aminoglycosides (gentamycin and tobramycin) and fluoroquinolones (ciprofloxacin and norfloxacin). Interpretation of antimicrobial susceptibility was based on European Committee on Antimicrobial Susceptibility Testing (EUCAST) 2017 guidelines [28].

3.1. Susceptibility of bacterial isolates to SET-M33 and colistin – minimum inhibitory concentration MIC

The susceptibility of the colistin-susceptible *K. pneumoniae* B-DYK 4861 and *P. aeruginosa* B-162 isolates and their colistin-resistant mutants to SET-M33 and colistin in terms of MIC are shown in Table 1.

3.2. SET-M33 and colistin activity against colistin-susceptible and colistin-resistant K. pneumoniae B-DYK 4861 and P. aeruginosa B-162 – time-kill-kinetics TKK

The major killing effect of an antibiotic against an organism depends on the exposure time or concentration of the drug at the active target site. In the present study we investigated extensively drug-resistant *K.*

Table 1
MICs of SET-M33 and colistin for bacterial isolates in triplicate.

Bacterial isolate		Colistin-susceptible *K. pneumoniae* R-DYK 4861		Colistin-resistant *K. pneumoniae* R-DYK 4861		Colistin-susceptible *P. aeruginosa* B-162		Colistin-resistant *P. aeruginosa* B-162	
AMP		Median	Range	Median	Range	Median	Range	Median	Range
SET-M33	mg/L	16	16–16	16	16–32	16	8–16	16	8–16
	μM	2.7	2.7–2.7	2.7	2.7–5.5	2.7	1.4–2.7	2.7	1.4–2.7
Colistin	mg/L	0.50	0.25–0.50	>512	>512	2	2–2	512	128–512
	μM	0.22	0.11–0.22	>222	>222	0.87	0.87–0.87	222	55–222

Colistin resistance did not affect SET-M33 susceptibility in these two strains, confirming our previous data on seven different colistin-resistant *K. pneumoniae* strains [21].
SET-M33 showed a MIC of 8 mg/L for *K. pneumoniae* ATCC 13833 and *P. aeruginosa* PAO1 [21].

pneumoniae and *P. aeruginosa* populations, taking the effects of exposure time and concentration into account.

Colistin-susceptible and colistin-resistant *K. pneumoniae* isolates were killed by ≥99.9% after 2 h of exposure to ≥4 mg/L and ≥8 mg/L SET-M33, respectively (the first concentration above the grey shade in Fig. 2A, B). This was followed by bacterial re-growth up to the level of non-exposed bacteria after 24 h exposure to ≤4 mg/L and ≤16 mg/L, respectively. Colistin killed ≥99.9% of the colistin-susceptible *K. pneumoniae* isolate after 2 h of exposure to ≥0.5 mg/L (Fig. 2C) and bacterial re-growth after 24 h exposure was observed up to ≤32 mg/L.

In the colistin-resistant isolate, colistin concentration-dependent killing was observed in the first hour of exposure but ≥99.9% killing was not achieved after 2 h of exposure (Fig. 2D).

For *P. aeruginosa*, ≥99.9% killing was achieved in colistin-susceptible and colistin-resistant isolates after 2 h of exposure to ≥8 mg/L SET-M33 (Fig. 2E and F).

Colistin killed ≥99.9% of bacteria in the colistin-susceptible *P. aeruginosa* isolate after 2 h of exposure to a concentration ≥ 1 mg/L (Fig. 2G). In the colistin-resistant *P. aeruginosa* isolate, colistin concentration-dependent killing was observed in the first 2 h of exposure, followed by bacterial re-growth up to the level of non-exposed bacteria after 24 h, at all the colistin concentrations tested (Fig. 2H).

We also showed that exposure to SET-M33 sterilized colistin-susceptible *K. pneumoniae* and *P. aeruginosa* populations already at one-fold (16 mg/L) (Fig. 2A) and four-fold (64 mg/L) (Fig. 2E) the MICs, respectively. In contrast, after exposure to colistin, sterilization only occurred at the extremely high concentration of 64 mg/L (Fig. 2C and G), which is 128-fold and 32-fold the MICs of colistin-susceptible *K. pneumoniae* and *P. aeruginosa*, respectively. Colistin-resistant *K. pneumoniae* and *P. aeruginosa* were sterilized with 64 mg/L SET-M33 (Fig. 2B and F) in both cases (four-fold the MIC) but never with colistin (Fig. 2D and H).

SET-M33 and colistin showed concentration-dependent bactericidal activity against colistin-susceptible and colistin-resistant isolates of *K. pneumoniae* and *P. aeruginosa*. This result is similar to the action of different widely used antibiotics e.g. aminoglycosides and fluoroquinolones, as well as other AMPs [31].

SET-M33 retains activity against both colistin-susceptible and colistin-resistant bacteria. This result indicates that SET-M33 is impervious to the mechanisms associated with colistin resistance.

3.3. Selection of resistance

Selection of resistance was assessed in the same experiments: when re-growth was observed after 24 h of exposure to antibiotic, bacterial susceptibilities were determined as MIC. Re-growth of colistin-susceptible strains of *K. pneumoniae* and *P. aeruginosa* after 24 h of exposure to SET-M33 was never associated with selection of SET-M33 resistance (Table 2): in fact, MIC values did not increase more than 0.5–2 fold, whereas re-growth of *K. pneumoniae* after 24 h of colistin exposure was associated with decreased susceptibility and a manifold increase in MIC (Table 2). Colistin was more effective against *P. aeruginosa*, although bacteria regrowing at 1 mg/L colistin showed a ~ six-fold increase in MIC.

Similar results were obtained with the colistin-resistant strains, although re-growth of colistin-resistant *K. pneumoniae* showed slightly lower susceptibility to SET-M33 with a four-fold increase in MIC (Table 2S Supplementary data).

Gram-negative bacteria can reduce their susceptibility to AMPs by reducing their net negative surface charges, modifying capsule polysaccharides, or reducing outer membrane fluidity [32]. In contrast to colistin, resistance to SET-M33 does not readily develop during 24 h of continuous exposure. This finding provides evidence that some of the resistance mechanisms that affect colistin do not affect SET-M33 to the same extent. For example, the mutations that lead to colistin resistance may not have the same effect on the activity of SET-M33, or alternatively, exposure to SET-M33 may not elicit the type of resistance mutations that are selected or induced by colistin. Ways of avoiding resistance will be investigated in further studies. Importantly, the fact that resistance to SET-M33 does not appear within 24 exposure period to the antibiotic provides evidence that the use of SET-M33 in the clinic may have advantages over the use of colistin. For example, colistin is currently used as an antibiotic of last resort for MDR bacteria [33–34], but besides its toxic side effects, it is also becoming dangerously more often ineffective due to increasing number of resistant strains [35–37].

3.4. Electron microscopy

The effect of SET-M33 treatment at MIC (8 mg/L SET-M33) for 15, 30 and 60 min on bacterial cell morphology was studied by scanning electron microscopy (SEM) and transmission electron microscopy (TEM). SEM images showed that after 30 min of SET-M33 treatment, the surfaces of *K. pneumoniae* ATCC 13833 and *P. aeruginosa* PAO1 cells lost their smoothness and developed superficial blisters (Fig. 3). After 60 min of SET-M33 treatment, bacterial cells appeared larger than control cells and many were empty and showed large holes, mainly at the poles.

TEM microscopy (Fig. 4) showed significant signs of alteration in most bacterial cells after 30 min of SET-M33 treatment: *P. aeruginosa* and *K. pneumoniae* cells appeared turgid and filamentous material appears on the external side of the outer membrane.

In the first 30 min after incubation with SET-M33, only a few *K. pneumoniae* and *P. aeruginosa* bacterial cells (rare in the micrograph field) showed cell damage.

Some linear peptides are reported to kill bacteria very quickly [16], while others, such as magainin-2, kill bacteria after 15–90 min. SET-M33 damages bacteria in the latter time range: indeed microscopy only showed initial signs of bacterial membrane disturbance in very few cells after 10–15 min of exposure. With longer exposure, the damage to bacterial membranes increased in frequency and severity.

3.5. Peptide conformation – NMR structure analysis and circular dichroism

The supramolecular structure of peptides is important and has been extensively studied in interactions of peptides with bacterial

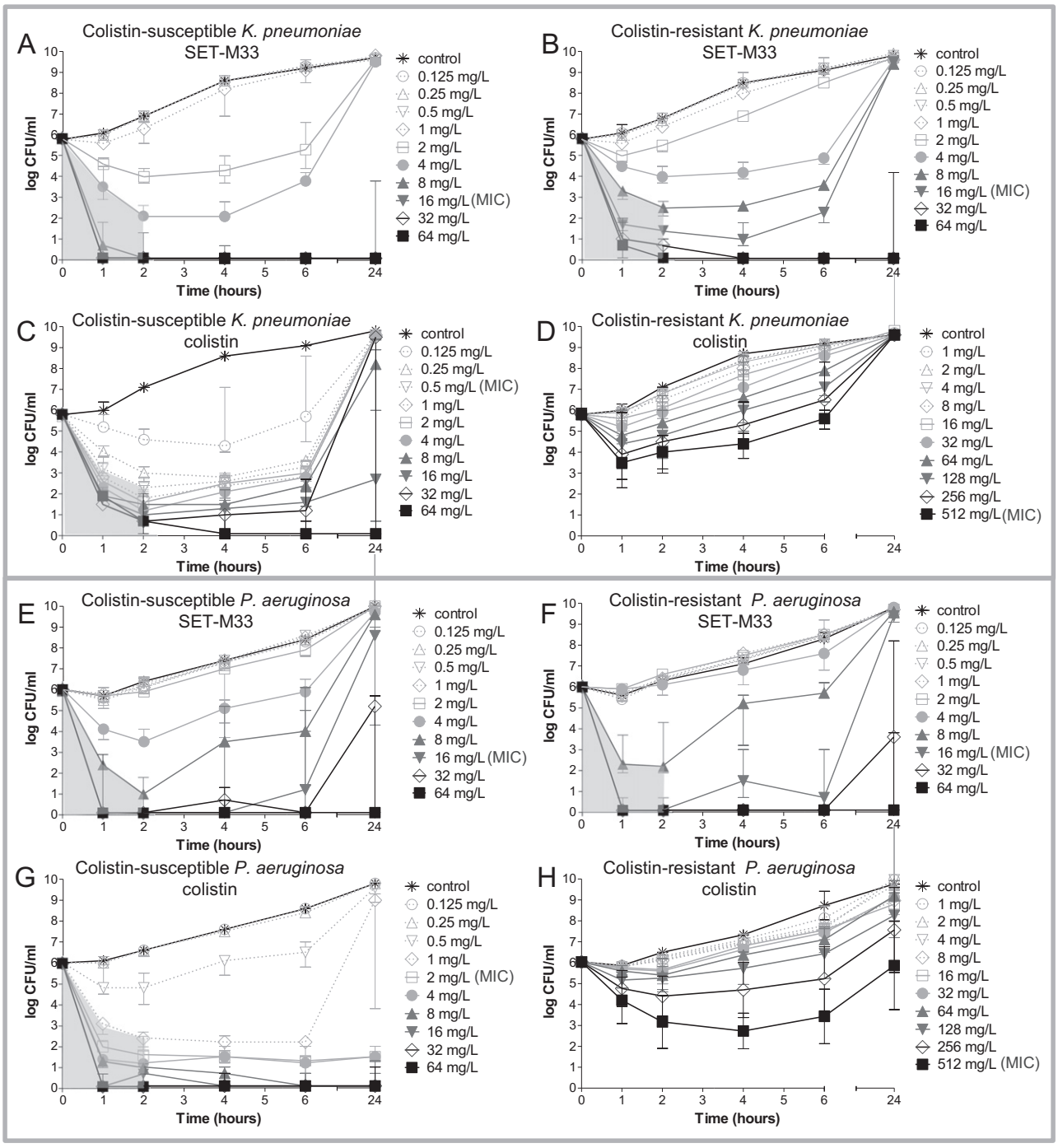

Fig. 2. Concentration- and time-dependent bactericidal activity of SET-M33 and colistin against isolates of *K. pneumoniae* R-DYK 4861 (A-D) and *P. aeruginosa* B-162 (E-H). Bacterial cultures were exposed to two-fold increasing concentrations of SET-M33 or colistin for 24 h at 37 °C under shaking conditions. Samples were collected at 1, 2, 4, 6 and 24 h, and after centrifuging and washing, were sub-cultured onto antibiotic-free solid media to determine CFU counts after incubation for 24 h at 37 °C. Data are medians of 3 experiments. Grey shading indicates ≥99.9% killing achieved after 2 h of exposure.

membranes [16,38–39]. The NMR spectra of free SET-M33 showed a chemical shift index typical of a random coiled conformation and no significant inter-residue NOEs, indicating that the peptide explores a large conformational space. On addition of sodium dodecyl sulfate (SDS) micelles, the NMR spectrum of SET-M33 undergoes a generalized broadening, caused by the production of slow-tumbling high-mass species, precluding further analysis. The high-mass species could be aggregates of SET-M33-SDS, possibly promoted by the multimericity of SET-M33. We therefore synthesized an analogue peptide, Q-33, in linear form and capped it with an additional amino acid (Q-KKIRVRLSA) at the N-terminus in order to generate a model of SET-M33 that could be studied in the presence of SDS. Q-33 has an extremely lower half life in serum and plasma than SET-M33, 2 h versus 24 h, and consistently it has a lower activity against Gram-negative bacteria [40–41]. The additional Q allowed us to study the structure of all residues, including the first lysine. Q-33 did not show any stable conformation in water, but addition of SDS micelles caused a generalized dispersion of proton resonances and the emergence of NOE peaks, indicating that a stable conformer was present as a consequence of the peptide-micelle interaction. In particular, NOE signals of the Hαi-HN_{i+3}, Hαi-$Hβ_{i+3}$ and HNi-HN_{i+2} types for residue $i = 1$ to 6 are diagnostic of α-helix conformation spanning residues 1–9 (Fig. 5A). Peak integration of a total set of 32 NOEs allowed

Table 2
Change in colistin-susceptible *K. pneumoniae* R-DYK 4861 and *P. aeruginosa* B-162 susceptibility to SET-M33 and colistin after 24 h exposure to antibiotic as determined by MIC assay.

Antibiotic concentration (mg/L)	SET-M33 (mg/L)		Colistin (mg/L)	
	Colistin-susceptible *K. pneumoniae*	Colistin-susceptible *P. aeruginosa*	Colistin-susceptible *K. pneumoniae*	Colistin-susceptible *P. aeruginosa*
Control	16	16	0.5	2
0.125	16	16	>64	2
0.25	16	16	>64	2
0.5	16	16	>64	4
1	16	16	>64	12[a]
2	16	16	>64	NR
4	32	16	>64	NR
8	NR	16	64[a]	NR
16	NR	12[a]	>64[b]	NR
32	NR	NR	>64[a]	NR
64	NR	NR	NR	NR

Colistin-susceptible bacterial cultures were exposed to two-fold increasing concentrations of SET-M33 or colistin for 24 h at 37 °C under shaking conditions. When bacteria re-grew after 24 h exposure to antibiotic, their MIC susceptibilities (performed in triplicate) were also determined and the median value reported. NR, no bacterial re-growth.
[a] One out of three samples did not show bacterial re-growth.
[b] Two out of three samples did not show bacterial re-growth.

us to calculate the relative interproton distances, which were used as constraints for simulation of torsion angle dynamics and subsequent peptide structure calculations. The resulting structure showed a regular α-helix encompassing the full-length of the peptide.

To assess the interaction geometry of the helix with SDS micelles, a paramagnetic solution-NMR experiment was performed. TOCSY (total correlation spectroscopy) spectra of the peptide-micelle system were acquired in the presence and absence of increasing concentrations of the paramagnetic probe Gd(III)(DTPA-BMA). The soluble probe causes nuclear spin relaxation proportional to the local surface accessibility of the molecule investigated [42–44]. Relaxation is measured by calculating the decrease in peak volumes on addition of the probe, and is summarized as a bare number, the attenuation value A, which ranges from 0 to 2 and can be determined for each known proton peak. Protons shielded by contact with the solvent, and therefore not accessible to the probe, show low A values, while exposed protons show high A values (Fig. 5B, upper part). Attenuation analysis was carried out on the Q-33-micelle system and an accurate accessibility profile was determined. Residues I3 and L7 showed much lower accessibility of the probe to their sidechains, and this can be ascribed to shielding by close interaction with the micelle surface. Charged residue pairs K1/R4 and K2/R6, situated on the opposite side of the helix, showed a higher A value, while V5 and S8 showed the highest attenuation due to their high exposure to the solvent. The resulting structure was a helix lying on the micelle surface with I3/L7 sidechains inserted into the SDS assembly, and R and K sidechains arranged parallel to the surface, their charged tips interacting with the negative sulfate groups (Fig. 5B). This facial amphiphilic structure has already been reported for other positively charged peptides [45], such as LL37 fragments [46] and CRAMP [47].

Finally, we wanted to assess whether SET-M33 and Q-33 had the same ability to adopt a helix conformation in a membrane mimicking environment, using circular dichroism. The technique proved to be applicable to both the tetrabranched and the linear peptide. SET-M33 and Q-33 CD spectra were recorded at room temperature in water and in SDS 30 mM. In line with the NMR experiments, SET-M33 showed a non-structured conformation in water but the CD spectrum shifted sharply to longer wavelengths in the presence of SDS micelles (Fig. 5C), and the calculated helix ratio switched from 0% to 30%. A similar result was obtained with Q-33 (Fig. 5D): the spectra recorded in water

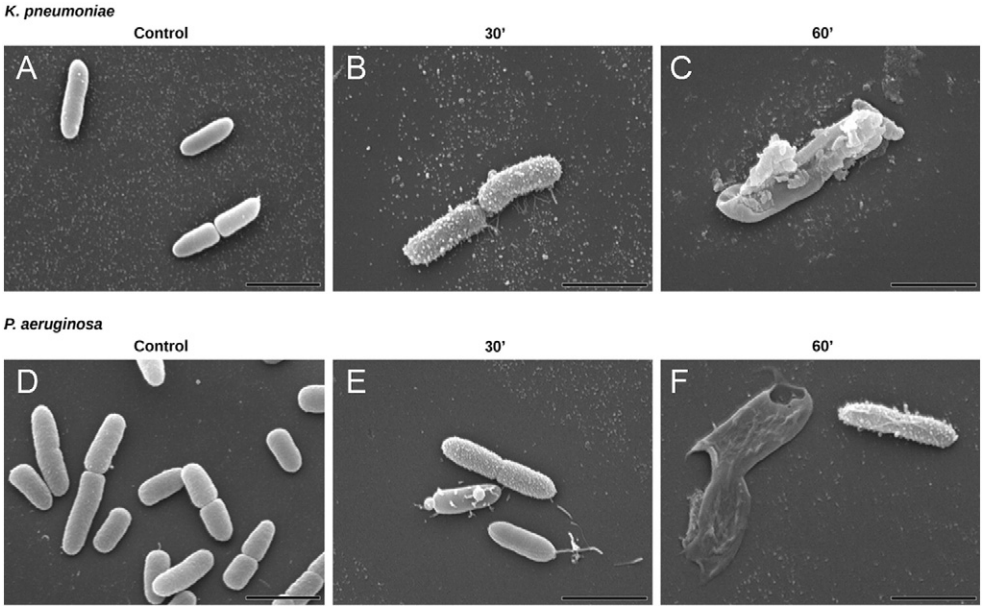

Fig. 3. Scanning electron micrographs (SEM) of *K. pneumoniae* ATCC 13833 and *P. aeruginosa* PAO1. SEM micrographs of A) untreated *K. pneumoniae*; B) *K. pneumoniae* after 30 min incubation with SET-M33 at MIC; C) *K. pneumoniae* after 60 min incubation with SET-M33 at MIC; D) untreated *P. aeruginosa*; E) *P. aeruginosa* after 30 min incubation with SET-M33 at MIC; F) *P. aeruginosa* after 60 min incubation with SET-M33 at MIC. Scale bar 2 μm.

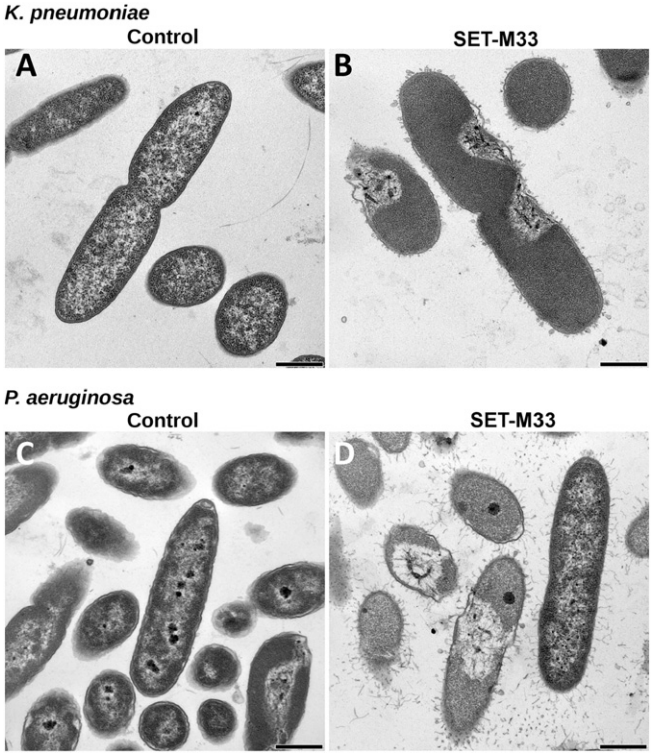

Fig. 4. Transmission electron micrographs (TEM) of *K. pneumoniae* ATCC 13833 and *P. aeruginosa* PAO1. TEM micrographs of A) untreated *K. pneumoniae*; B) *K. pneumoniae* after 60 min incubation with SET-M33 at MIC; C) untreated *P. aeruginosa*; D) *P. aeruginosa* after 60 min incubation with SET-M33 at MIC. Scale bar 500 nm.

had a calculated helix ratio of 3.3% compared to 39% in the presence of SDS micelles. The CD spectra of SET-M33 and Q-33, recorded with or without micelles, were very similar, confirming that Q-33 was a reliable model of SET-M33 for the NMR experiments.

3.6. Selectivity/hemolytic activity

The ability of cationic peptides to stabilize as an α-helix, and particularly as a facial amphiphilic structure, is often associated with self-aggregation and undesired peptide interactions with blood proteins due to exposed hydrophobic surfaces [45]. The tendency to self-aggregate is correlated to hydrophobicity and provides an indirect estimate of the propensity for partitioning into lipid membranes with unselective detergent-like characteristics. Antimicrobial peptides need to be selective for prokaryotic membranes; a well-established method of verifying their ability to damage eukaryotic cell membranes is to measure their hemolytic activity [48]. Our results showed that red blood cells incubated with increasing concentrations of SET-M33 did not show more than 26% lysis, even using a concentration of 1.8 mg/mL (320 μM), which is > 100-fold the MIC (Fig. 6).

In contrast with other cationic peptides [49], SET-M33 showed very little hemolytic activity against red blood cells, although it shares the ability to form a regular α-helix shape. Indeed, SET-M33 also proved not to be cytotoxic to human bronchial epithelial cells (16HBE14 and CFBE41) [23]. Self-aggregation, often associated with amphiphilic structures and undesired secondary effects [49], was also studied in FPLC experiments (Supplementary material – Fig. 1S, A) and showed that no self-aggregation occurred when SET-M33 was dissolved in PBS. The presence of LPS promoted the formation of high-mass hetero-multimers, but not homo-multimers (Supplementary material – Fig. 1S, B), in line with what we observed and described above in relation to SDS.

4. Conclusions

Current understanding of the mechanism of action of cationic AMPs includes a first step of electrostatic attraction between the cationic peptide and the negatively charged bacterial outer membrane. As SET-M33 is a cationic amphiphilic peptide it is attracted to the negatively charged bacterial membrane. Once close to the microbial surface, AMPs need to cross the polysaccharide cell wall barrier before interacting with the

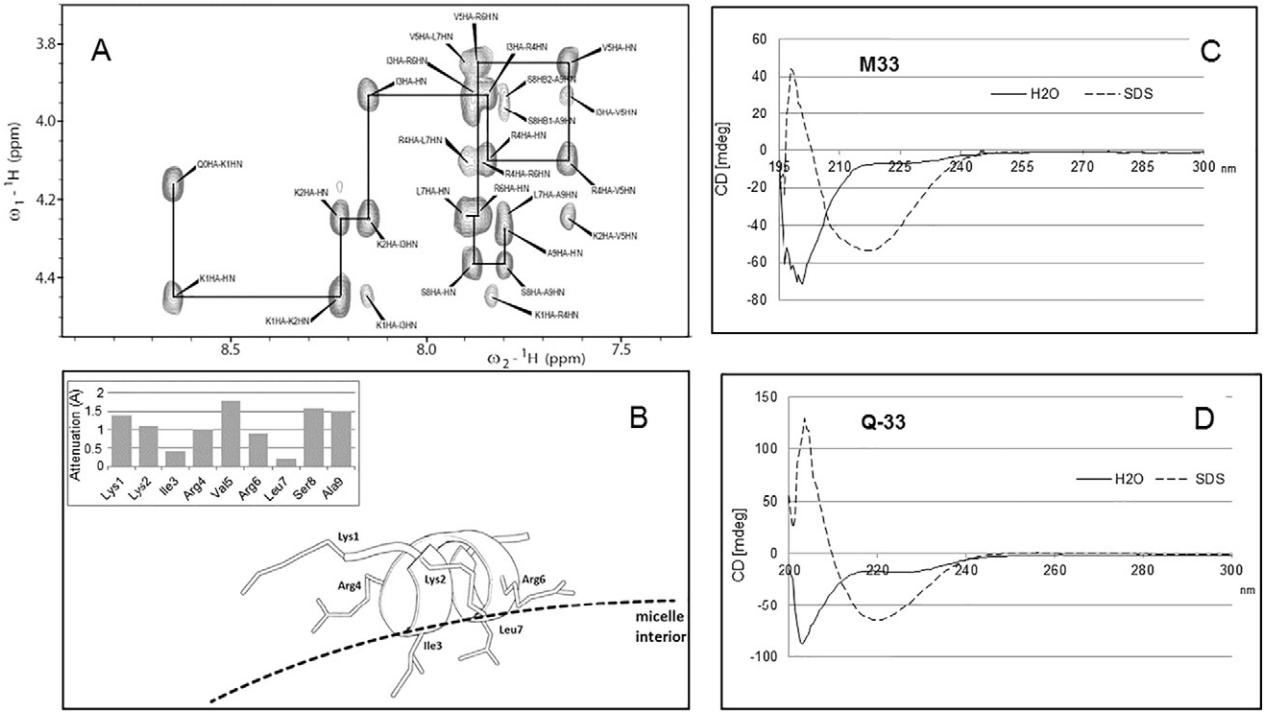

Fig. 5. A) NOESY spectrum of Q-33 peptide in the presence of SDS micelles showing the Hα-HN correlation path typical of α-helices. B) Structural model of peptide conformation and interaction geometry with micelle surface (dashed line) as derived from NMR data, attenuation values A obtained by adding the soluble paramagnetic probe Gd(III)(DTPA-BMA) to the peptide/SDS sample are reported in the upper part. C) CD spectrum of SET-M33100 μM in water and SDS 30 mM. D) CD spectrum of Q-33100 μM in water and SDS 30 mM.

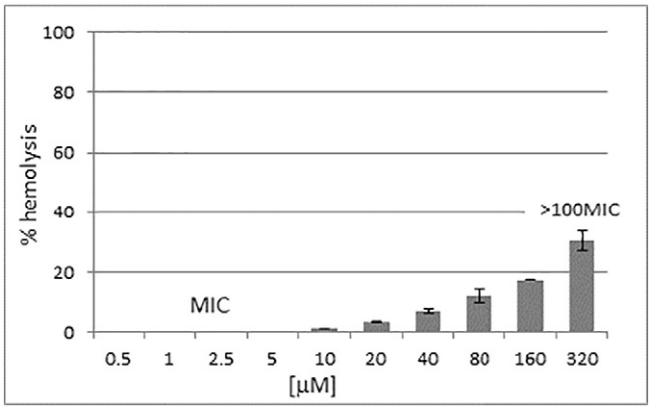

Fig. 6. Hemolytic activity of SET-M33. Percentage of red blood cell hemolysis after 24 h incubation at 37 °C. The range of MIC90 for *K. pneumoniae* and *P. aeruginosa* is indicated.

cytoplasmic membrane [15,50–51]. In line with this, in previous studies, SET-M33 was shown, by surface plasmon resonance, to bind LPS of *K. pneumoniae* and *P. aeruginosa* [52] and the binding prevented TNF-α release, neutralizing endotoxin activity *in vitro* and *in vivo* [22,41]. In the present study, NMR investigation of Q-33/SDS micelles in solution and in the presence of a paramagnetic probe showed that the α-helix arranges itself on the surface of micelles as previously described for other antimicrobial peptides [53–55]. Though direct measurement of the geometry of SET-M33/SDS micelle interactions was not possible, we demonstrated with CD that the structural transition observed using Q-33/SDS micelles also occurs using the original tetra-branched SET-M33 peptide. The α-helix showed to be partially buried in the lipid-bilayer. In the course of 15–60 min, the signs of membrane damages are, indeed, evident in electron microscopy. We also knew that SET-M33 is internalized in *E. coli* within 5 min, proving that it can cross cell wall and plasma membranes [41], causing enhanced membrane permeability, as observed with fluorescent probes [41]. Bacteria death may realistically be caused by impairment of the membrane homeostasis and functionality.

Interestingly, SET-M33 is different from other α-helix antimicrobial peptides in that it shows little propensity to self-aggregate and also no hemolytic activity. Homo-aggregation, which is considered related with undesired toxicity [48–49], is never observed. This aspect probably contributes in preventing non-specific interactions with eukaryotic cells [48–49] and indeed correlates with an acceptable tolerability profile obtained in toxicology studies in mice [21].

SET-M33 does not show any cross-resistance with colistin in colistin-resistant bacteria and, differently from colistin, it appears to generate substantially no resistance within 24 h of exposure in extensively resistant isolates of *K. pneumoniae* and *P. aeruginosa*. These observations suggest that the two peptides have a different mechanism of action. SET-M33 is attracted onto the surface of bacteria by the anionic charges of the cell wall. Being the core of the branched peptide completely flexible, we speculate that in the presence of phospholipid-bilayers, the peptide can assume a star like conformation, where hydrophobic residues are buried in the surface and hydrophilic residues point outwards. The disturbance of bilayers integrity, produced by SET-M33's peculiar way to interact with membranes, makes it more difficult for bacteria to trigger resistance mechanisms than it is for colistin.

Finally SET-M33, in contrast to other similar antimicrobial peptides such as colistin, does not generate resistant mutants after 24 h of exposure, and non-specific interactions or toxicity against eukaryotic cell membranes, suggesting that SET-M33 is a promising new option for the treatment of Gram-negative antibiotic-resistant infections.

Funding

Setlance srl and Erasmus University Medical Center Rotterdam received funding from the European Union's Seventh Programme for Research, Technological Development and Demonstration under grant agreement No. 604434 (PNEUMO-NP). A.P. received funding from the Italian Foundation for Cystic Fibrosis (Project FFC#17/2016).

Transparency declarations

Chiara Falciani, Alessandro Pini and Luisa Bracci are cofounders of Setlance srl. SET-M33 is owned by Setlance srl.

Transparency document

The Transparency document associated with this article can be found, in online version.

Acknowledgements

We thank Silvia Scali for qualified assistance with peptide synthesis and Giacomo Landi for support with FPLC chromatography.

Appendix A. Supplementary data

Supplementary data to this article can be found online at http://dx.doi.org/10.1016/j.bbamem.2017.06.001.

References

[1] G. Kahlmeter, An international survey of the antimicrobial susceptibility of pathogens from uncomplicated urinary tract infections: the ECO·SENS Project, J. Antimicrob. Chemother. 51 (2003) 69–76.
[2] J.D. Chalmers, C. Rother, W. Salih, S. Ewig, Healthcare-associated pneumonia does not accurately identify potentially resistant pathogens: a systematic review and meta-analysis, Clin. Infect. Dis. 58 (2014) 330–339.
[3] I. Karaiskos, H. Giamarellou, Multidrug-resistant and extensively drug-resistant Gram-negative pathogens: current and emerging therapeutic approaches, Expert. Opin. Pharmacother. 15 (2014) 1351–1370.
[4] R.J. Fair, Y. Tor, Antibiotics and bacterial resistance in the 21st century, Perspect. Med. Chem. 6 (2014) 25–64.
[5] L.L. Maragakis, E.N. Perencevich, S.E. Cosgrove, Clinical and economic burden of antimicrobial resistance, Expert Rev. Anti-Infect. Ther. 6 (2008) 751–763.
[6] World Health Organization, Antimicrobial Resistance: Global Report on Surveillance, World Health Organization, 2014.
[7] R.E. Hancock, H.G. Sahl, Antimicrobial and host-defense peptides as new anti-infective therapeutic strategies, Nat. Biotechnol. 24 (2006) 1551–1557.
[8] C. de la Fuente-Núñez, O.N. Silva, T.K. Lu, Antimicrobial peptides: Role in human disease and potential as immunotherapies, Pharmacol Ther. (2017) pii: S0163-7258(17)30105-5.
[9] E.F. Haney, S.C. Mansour, R.E. Hancock, Antimicrobial peptides: an introduction, Methods Mol. Biol. 1548 (2017) 3–22.
[10] L.J. Zhang, R.L. Gallo, Antimicrobial peptides, Curr. Biol. 26 (2016) R14–R19.
[11] G. Roscia, C. Falciani, L. Bracci, A. Pini, The development of antimicrobial peptides as new antibacterial drugs, Curr. Protein Pept. Sci. 14 (2013) 641–649.
[12] J. Brunetti, C. Falciani, L. Bracci, A. Pini, Models of in-vivo bacterial infections for the development of antimicrobial peptide-based drugs, Curr. Top. Med. Chem. 17 (2017) 613–619.
[13] R.M. Epand, H.J. Vogel, Diversity of antimicrobial peptides and their mechanisms of action, Biochim. Biophys. Acta 1462 (1999) 11–28.
[14] B. Bechinger, K. Lohner, Detergent-like actions of linear amphipathic cationic antimicrobial peptides, Biochim. Biophys. Acta 1758 (2006) 1529–1539.
[15] T.P. Cushnie, N.H. O'Driscoll, A.J. Lamb, Morphological and ultrastructural changes in bacterial cells as an indicator of antibacterial mechanism of action, Cell. Mol. Life Sci. 73 (2016) 4471–4492, http://dx.doi.org/10.1007/s00018-016-2302-2.
[16] K.A. Brogden, Antimicrobial peptides: pore formers or metabolic inhibitors in bacteria? Nat. Rev. Microbiol. 3 (2005) 238–250.
[17] M. Wilmes, B.P. Cammue, H.G. Sahl, Antibiotic activities of host defense peptides: more to it than lipid bilayer perturbation, Nat. Prod. Rep. 28 (2011) 1350–1358.
[18] G. Bierbaum, H.G.L. Sahl, Antibiotics: mode of action, biosynthesis and bioengineering, Curr. Pharm. Biotechnol. 10 (2009) 2–18.
[19] R.M. Epand, R.F. Epand, Bacterial membrane lipids in the action of antimicrobial agents, J. Pept. Sci. 17 (2011) 298–305.
[20] R.M. Epand, R.F. Epand, Domains in bacterial membranes and the action of antimicrobial agents, Mol. BioSyst. 5 (2009) 580–587.
[21] S. Pollini, J. Brunetti, S. Sennati, G.M. Rossolini, L. Bracci, A. Pini, C. Falciani, Synergistic activity profile of an antimicrobial peptide against multidrug-resistant and

extensively drug-resistant strains of Gram-negative bacterial pathogens, J. Pept. Sci. 23 (2017) 329–333, http://dx.doi.org/10.1002/psc.2978.
[22] J. Brunetti, C. Falciani, G. Roscia, S. Pollini, S. Bindi, S. Scali, U.C. Arrieta, V. Gómez-Vallejo, L. Quercini, E. Ibba, M. Prato, G.M. Rossolini, J. Llop, L. Bracci, A. Pini, In vitro and in vivo efficacy, toxicity, bio-distribution and resistance selection of a novel antibacterial drug candidate, Sci. Rep. 6 (2016) 26077, http://dx.doi.org/10.1038/srep26077.
[23] J. Brunetti, G. Roscia, I. Lampronti, R. Gambari, L. Quercini, C. Falciani, L. Bracci, A. Pini, Immunomodulatory and anti-inflammatory activity in vitro and in vivo of a novel antimicrobial candidate, J. Biol. Chem. 291 (2016) 25742–25748.
[24] A. Pini, L. Lozzi, A. Bernini, J. Brunetti, C. Falciani, S. Scali, S. Bindi, T. Di Maggio, G.M. Rossolini, N. Niccolai, L. Bracci, Efficacy and toxicity of the antimicrobial peptide M33 produced with different counter-ions, Amino Acids 43 (2012) 467–473.
[25] A. Pini, C. Falciani, E. Mantengoli, S. Bindi, J. Brunetti, S. Iozzi, G.M. Rossolini, L. Bracci, A novel tetrabranched antimicrobial peptide that neutralizes bacterial lipopolysaccharide and prevents septic shock in vivo, FASEB J. 24 (2010) 1015–1022.
[26] L. Bracci, C. Falciani, B. Lelli, L. Lozzi, Y. Runci, A. Pini, M.G. De Montis, A. Tagliamonte, P. Neri, Synthetic peptides in the form of dendrimers become resistant to protease activity, J. Biol. Chem. 278 (2003) 46590–46595.
[27] X. Vila-Farrés, M. Ferrer-Navarro, A.E. Callarisa, S. Martí, P. Espinal, S. Gupta, J.M. Rolain, E. Giralt, J. Vila, Loss of LPS is involved in the virulence and resistance to colistin of colistin-resistant *Acinetobacter nosocomialis* mutants selected in vitro, J. Antimicrob. Chemother. 70 (2015) 2981–2986.
[28] The European Committee on Antimicrobial Susceptibility Testing, Breakpoint tables for interpretation of MICs and zone diameters, Version 7.1 (2017) http://www.eucast.org.
[29] J.E. de Steenwinkel, G.J. de Knegt, M.T. ten Kate, A. van Belkum, H.A. Verbrugh, K. Kremer, D. van Soolingen, I.A. Bakker-Woudenberg, Time-kill kinetics of anti-tuberculosis drugs, and emergence of resistance, in relation to metabolic activity of *Mycobacterium tuberculosis*, J. Antimicrob. Chemother. 65 (2010) 2582–2589.
[30] P. Güntert, C. Mumenthaler, K. Wüthrich, Torsion angle dynamics for NMR structure calculation with the new program DYANA, J. Mol. Biol. 273 (1997) 283–298.
[31] H.W. Lampiris, D.S. Maddix, Clinical use of antimicrobial agents (chapter 51), in: B.G. Katzung, S.B. Masters, A.J. Trevor (Eds.),Basic and Clinical Pharmacology, 2012.
[32] M.A. Campos, M.A. Vargas, V. Regueiro, C.M. Llompart, S. Albertí, J.A. Bengoechea, Capsule polysaccharide mediates bacterial resistance to antimicrobial peptides, Infect. Immun. 72 (2004) 7107–7114.
[33] J. Li, R.L. Nation, J.D. Turnidge, R.W. Milne, K. Coulthard, C.R. Rayner, D.L. Paterson, Colistin: the re-emerging antibiotic for multidrug-resistant Gram-negative bacterial infections, Lancet Infect. Dis. 6 (2006) 589–601.
[34] N. Petrosillo, M. Giannella, M. Antonelli, M. Antonini, B. Barsic, L. Belancic, A.C. Inkaya, G. De Pascale, E. Grilli, M. Tumbarello, M. Akova, Clinical experience of colistin-glycopeptide combination in critically ill patients infected with Gram-negative bacteria, Antimicrob. Agents Chemother. 58 (2014) 851–858.
[35] Y.M. Ah, A.J. Kim, J.Y. Lee, Colistin resistance in *Klebsiella pneumoniae*, Int. J. Antimicrob. Agents 44 (2014) 8–15 (2014).
[36] C.G. Giske, Contemporary resistance trends and mechanisms for the old antibiotics colistin, temocillin, fosfomycin, mecillinam and nitrofurantoin, Clin. Microbiol. Infect. 21 (2015) 899–905.
[37] Y.Y. Liu, Y. Wang, T.R. Walsh, L.X. Yi, R. Zhang, J. Spencer, Y. Doi, G. Tian, B. Dong, X. Huang, L.F. Yu, D. Gu, H. Ren, X. Chen, L. Lv, D. He, H. Zhou, Z. Liang, J.H. Liu, J. Shen, Emergence of plasmid-mediated colistin resistance mechanism MCR-1 in animals and human beings in China: a microbiological and molecular biological study, Lancet Infect. Dis. 16 (2016) 161–168.
[38] R.E. Hancock, R. Lehrer, Cationic peptides: a new source of antibiotics, Trends Biotechnol. 16 (1998) 82–88.
[39] P. Kemayo Koumkoua, C. Aisenbrey, E. Salnikov, O. Rifi, B. Bechinger, On the design of supramolecular assemblies made of peptides and lipid bilayers, J. Pept. Sci. 20 (2014) 526–536.
[40] A. Pini, A. Giuliani, C. Falciani, Y. Runci, C. Ricci, B. Lelli, M. Malossi, P. Neri, G.M. Rossolini, L. Bracci, Antimicrobial activity of novel dendrimeric peptides obtained by phage display selection and rational modification, Antimicrob. Agents Chemother. 49 (2005) 2665–2672.
[41] A. Pini, A. Giuliani, C. Falciani, M. Fabbrini, S. Pileri, B. Lelli, L. Bracci, Characterization of the branched antimicrobial peptide M6 by analyzing its mechanism of action and in vivo toxicity, J. Pept. Sci. 13 (2007) 393–399.
[42] A. Bernini, O. Spiga, V. Venditti, F. Prischi, M. Botta, G. Croce, A.P. Tong, W.T. Wong, N. Niccolai, The use of a ditopic Gd(III) paramagnetic probe for investigating α-bungarotoxin surface accessibility, J. Inorg. Biochem. 112 (2012) 25–31.
[43] A. Bernini, L. Henrici De Angelis, E. Morandi, O. Spiga, A. Santucci, M. Assfalg, H. Molinari, S. Pillozzi, A. Arcangeli, N. Niccolai, Searching for protein binding sites from molecular dynamics simulations and paramagnetic fragment-based NMR studies, Biochim. Biophys. Acta 1844 (2014) 561–566.
[44] A. Bernini, V. Venditti, O. Spiga, A. Ciutti, F. Prischi, R. Consonni, L. Zetta, I. Arosio, P. Fusi, A. Guagliardi, N. Niccolai, NMR studies on the surface accessibility of the archaeal protein Sso7d by using TEMPOL and Gd(III)(DTPA-BMA) as paramagnetic probes, Biophys. Chem. 137 (2008) 71–75.
[45] M. Xiong, M.W. Lee, R.A. Mansbach, Z. Song, Y. Bao, R.M. Peek Jr., C. Yao, L.F. Chen, A.L. Ferguson, G.C. Wong, J. Cheng, Helical antimicrobial polypeptides with radial amphiphilicity, Proc. Natl. Acad. Sci. U. S. A. 112 (2015) 13155–13560.
[46] X. Li, Y. Li, H. Han, D.W. Miller, G. Wang, Solution structures of human LL-37 fragments and NMR-based identification of a minimal membrane-targeting antimicrobial and anticancer region, J. Am. Chem. Soc. 128 (2006) 5776–5785.
[47] K. Yu, K. Park, S.W. Kang, S.Y. Shin, K.S. Hahm, Y. Kim, Solution structure of a cathelicidin-derived antimicrobial peptide, CRAMP as determined by NMR spectroscopy, J. Pept. Res. 60 (2002) 1–9.
[48] E.J. Prenner, M. Kiricsi, M. Jelokhani-Niaraki, R.N. Lewis, R.S. Hodges, R.N. McElhaney, Structure-activity relationships of diastereomeric lysine ring size analogs of the antimicrobial peptide gramicidin S: mechanism of action and discrimination between bacterial and animal cell membranes, J. Biol. Chem. 280 (2005) 2002–2011.
[49] Z. Jiang, A.I. Vasil, M.L. Vasil, R.S. Hodges, "Specificity determinants" improve therapeutic indices of two antimicrobial peptides piscidin 1 and dermaseptin S4 against the Gram-negative pathogens *Acinetobacter baumannii* and *Pseudomonas aeruginosa*, Pharmaceuticals 7 (2014) 366–391.
[50] A. Datta, D. Bhattacharyya, S. Singh, A. Ghosh, A. Schmidtchen, M. Malmsten, A. Bhunia, Role of aromatic amino acids in lipopolysaccharide and membrane interactions of antimicrobial peptides for use in plant disease control, J. Biol. Chem. 291 (2016) 13301–13317, http://dx.doi.org/10.1074/jbc.M116.719575.
[51] A. Datta, A. Ghosh, C. Airoldi, P. Sperandeo, K.H. Mroue, J. Jiménez-Barbero, P. Kundu, A. Ramamoorthy, A. Bhunia, Antimicrobial peptides: insights into membrane permeabilization, lipopolysaccharide fragmentation and application in plant disease control, Sci. Rep. 5 (2015) 11951, http://dx.doi.org/10.1038/srep11951.
[52] C. Falciani, L. Lozzi, S. Pollini, V. Luca, V. Carnicelli, J. Brunetti, B. Lelli, S. Bindi, S. Scali, A. Di Giulio, G.M. Rossolini, M.L. Mangoni, L. Bracci, A. Pini, Isomerization of an antimicrobial peptide broadens antimicrobial spectrum to Gram-positive bacterial pathogens, PLoS One 7 (2012) e46259, http://dx.doi.org/10.1371/journal.pone.0046259.
[53] M. Hartmann, M. Berditsch, J. Hawecker, M.F. Ardakani, D. Gerthsen, A.S. Ulrich, Damage of the bacterial cell envelope by antimicrobial peptides gramicidin S and PGLa as revealed by transmission and scanning electron microscopy, Antimicrob. Agents Chemother. 54 (2010) 3132–3142.
[54] H. Sato, J.B. Feix, Peptide-membrane interactions and mechanisms of membrane destruction by amphipathic alpha-helical antimicrobial peptides, Biochim. Biophys. Acta 1758 (2006) 1245–1256.
[55] A.A. Bahar, D. Ren, Antimicrobial peptides, Pharmaceuticals 6 (2013) 1543–1575.